SAND75-0431
Unlimited Release

The Darrieus Turbine: A Performance Prediction Model Using Multiple Streamtubes

James H. Strickland

Prepared by Sandia Laboratories, Albuquerque, New Mexico 87115
and Livermore, California 94550 for the United States Energy Research
and Development Administration under Contract AT(29–1)-789

Printed October 1975

Sandia Laboratories
energy report

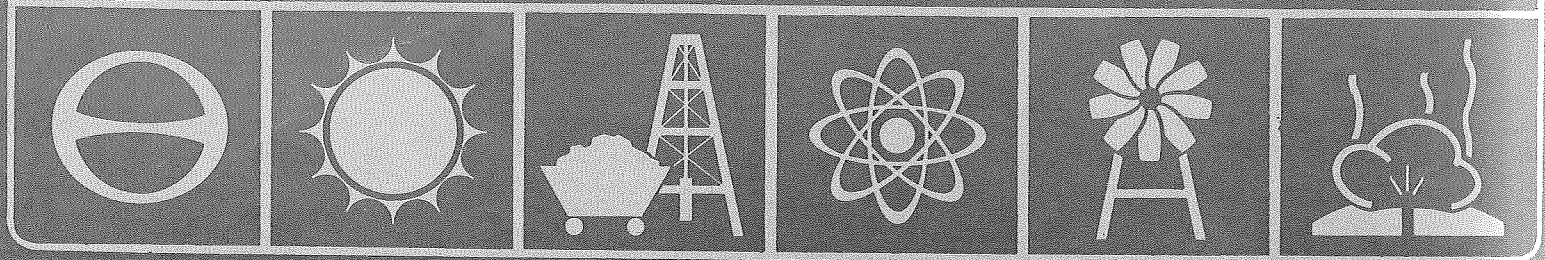

SAND75-0431
Unlimited Release

The Darrieus Turbine: A Performance Prediction Model Using Multiple Streamtubes

J. H. Strickland
Advanced Energy Projects Department, 5710*
Sandia Laboratories
Albuquerque, New Mexico 87115

October 1975

ABSTRACT

This report describes a multiple streamtube performance prediction model for the Darrieus turbine. This model is shown to predict the performance of small-scale rotors, for which test data is available, much more accurately than the single streamtube model. The model is capable of predicting the overall rotor power output and the distribution of aerodynamic forces along the rotor blades. The model can be used to study the effects of rotor geometry variations such as blade solidity, blade taper, and variations in rotor height-to-diameter ratios. In addition, spacial variations in freestream velocity such as that produced by atmospheric wind shear can be easily incorporated into the model. This model will assist in the proper design and optimization of large-scale rotors for which test data is not available. Scale effects can be predicted based upon the proper use of high Reynold's number airfoil data.

*Summer Faculty, Permanent Address: Department of Mechanical Engineering, Texas Tech University, Lubbock, TX 79409

Contents

		Page
1.0	Introduction	1
2.0	Aerodynamic Model	3
	2.1 Momentum Considerations	3
	2.2 Blade Element Forces	5
	2.3 Relative Velocity Vector	8
	2.4 Solution of the Momentum Equation	8
	2.5 Rotor Power Coefficient	10
3.0	Discussion of Results	12
	3.1 Comparison with Test Results	13
	3.2 Comparison with Single Streamtube Model	16
	3.3 Solidity and Reynold's Number Effects	16
	3.4 Blade Power Distribution	21
	3.5 Wind Shear Effects	21
4.0	DART Computer Model	23
	4.1 Input	23
	4.2 Output	25
	4.3 Computer Listing	27
5.0	Conclusions and Recommendations	29
	Bibliography	31

1.0 Introduction

Recent interest in the Darrieus Turbine as a wind energy conversion device [1-4] has resulted in a need for an adequate performance prediction model. Such a model is necessary so that large scale rotor systems can be properly engineered and optimized. This model must accurately predict the performance of small scale rotors, for which test data is currently available, if there is to be any hope of predicting the performance of large scale rotors whose blade Reynold's numbers are more than an order of magnitude greater.

There are several models from which one could select, ranging from very complex to reasonably simple. One could, for instance, attempt a solution using vortex theory, which has been successfully used in propellor and wing design. However, because of the complex structure of the resulting vortex system applicable to the Darrieus Turbine configuration, the computer time required to effect such a solution appears to be excessive. Another approach which has recently been used [5] is to visualize that the rotor is enclosed in a single streamtube. As this streamtube passes through the rotor, the wind velocity is assumed to be everywhere constant. The forces on the airfoil blades are then computed, using this uniform velocity. The wind velocity in the streamtube at the rotor is then related to the undisturbed freestream velocity by equating the drag force on the rotor to the change in fluid momentum through the rotor. While this approach is somewhat elegant in its simplicity and predicts overall performance rather well for lightly loaded blades, it is incapable of adequately predicting information which requires a more precise knowledge of wind velocty variations across the rotor. These

variations become increasingly large as blade solidities and blade tip speeds increase. In addition, it does not appear that wind shear effects can be incorporated into the model.

A somewhat more sophisticated model than the single streamtube model is one in which a series of streamtubes are assumed to pass through the rotor. The same basic principles which were applied to the single streamtube are now applied to each of the multiple streamtubes. The multiple streamtube model gives rise to a velocity distribution through the rotor which is a function of the two spacial coordinates perpendicular to the streamwise direction. The multiple streamtube model, while still somewhat inadequate in its description of the flow field, does predict overall performance very well, yields a more realistic distribution of blade forces, and can easily be modified to include wind shear effects.

This report consists of the development and utilization of the multiple streamtube model. The basic aerodynamic model is first developed along with a description of a suitable digital computer solution technique. The associated computer analysis is given the acronym DART for DARrieus Turbine. The DART model is exercised to provide comparison with test data and the single streamtube model. Effects of solidity and Reynold's number variations on overall performance are then investigated. The contribution of various blade segments to the overall power output and the effects of wind shear are investigated very briefly. Finally, suggestions are made concerning further utilization to provide additional engineering design information.

2.0 Aerodynamic Model

The performance analysis is based upon a simplified aerodynamic model which is an adaptation of Glauerts blade element theory [6]. Basically, this theory utilizes the streamwise momentum equation, which equates the streamwise forces on the airfoil blades to the change in fluid momentum through the rotor. Computations are performed for a series of streamtubes which pass through the rotor giving rise to a non-uniform distribution of fluid velocities through the rotor. The DART computer program is the computational vehicle for carrying out the calculations.

In figure 1 a typical streamtube is shown passing through the rotor. The cross-sectional area of the streamtube is given by $\Delta h r \Delta\theta \sin\theta$, where Δh is the vertical height of the streamtube. The streamtube cross-sectional area is assumed to be constant as it passes through the rotor, although it is apparent that it will diverge somewhat. The fluid velocity through the streamtube at the rotor is denoted by U and is a function of the angle θ and the vertical coordinate Z.

2.1 Momentum Considerations

Since energy is extracted by the blade elements as they pass through the streamtube, the rotor streamtube velocity U is less than the undisturbed freestream velocity U_∞. The time averaged streamwise momentum equation can be used in conjunction with Bernoulli's equation to relate the velocities U and U_∞ and the average streamwise force F_X exerted by the blade elements as they pass through the streamtube. This expression can be written as:

$$\bar{F}_X = 2 \rho A_S U (U_\infty - U) \qquad (1)$$

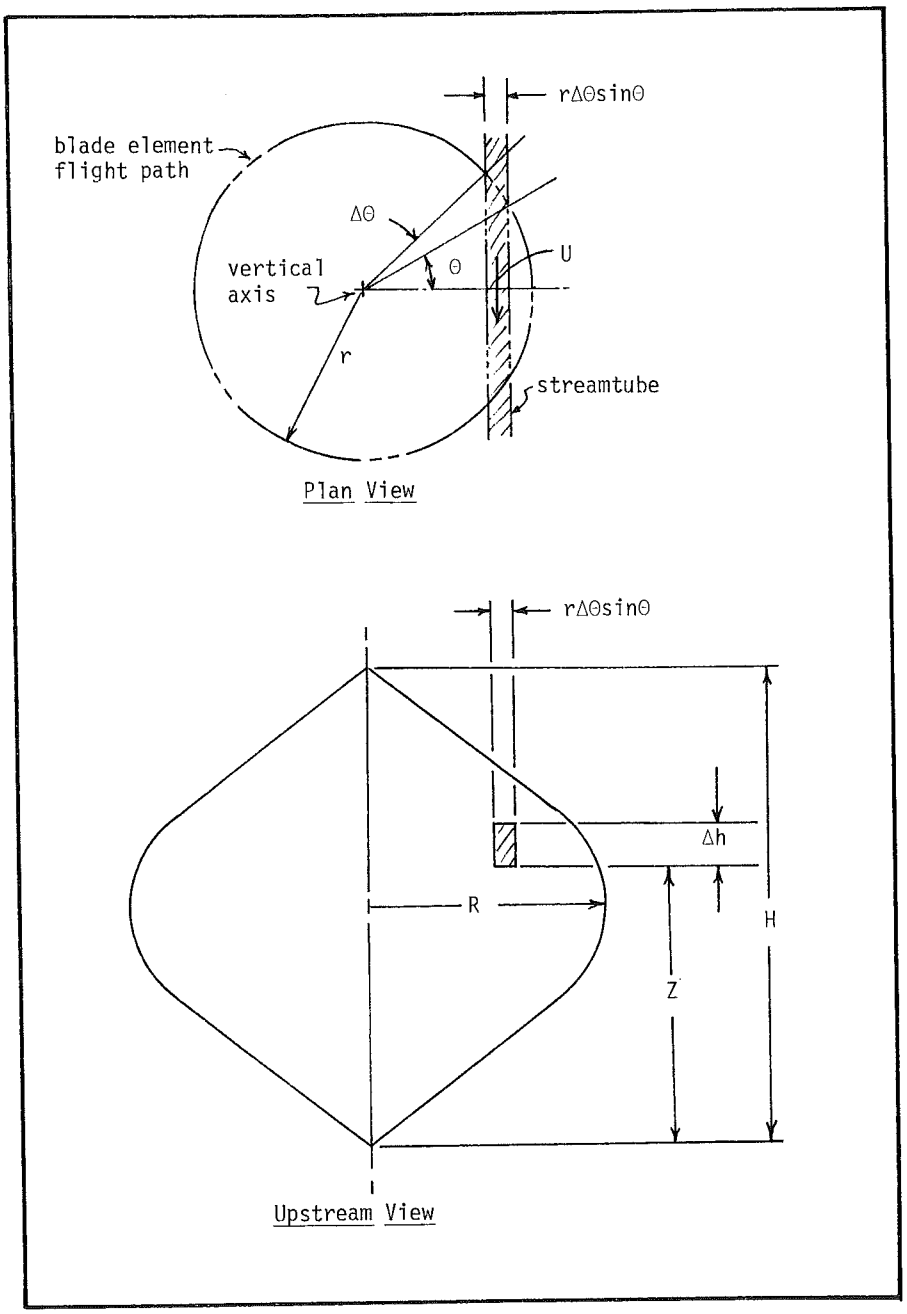

Figure 1 Typical Streamtube

where ρ is the fluid density and A_s is the streamtube cross-sectional area as defined previously.

The average force $\bar{F}_x$ in the streamtube can be related to the streamwise force F_x exerted by an individual blade element as it passes through the streamtube by noting that each of N blade elements spend $\Delta\theta/\pi$ percent of their time in the streamtube. Therefore the average force becomes:

$$\bar{F}_x = NF_x \frac{\Delta\theta}{\pi} \tag{2}$$

Eliminating $\bar{F}_x$ from equations 1 and 2 yields:

$$\frac{NF_x}{2\pi\rho r\Delta h \sin\theta U_\infty^2} = \frac{U}{U_\infty}\left(1 - \frac{U}{U_\infty}\right) \tag{3}$$

For convenience, the left hand side of equation 3 is denoted by F_x^*

$$F_x^* = \frac{NF_x}{2\pi\rho r\Delta h \sin\theta U_\infty^2} \tag{4}$$

2.2 Blade Element Forces

As seen from equation 3, the streamwise force exerted on the blade elements by the fluid must be found to obtain the ratio of rotor streamtube velocity to undisturbed freestream velocity. In addition, the force F_t, which acts along the chord line of the airfoil and tangential to the blade element flight path, must be found in order to compute the torque and power being produced by the element as it passes through the streamtube. A complete set of aerodynamic forces on a blade element would include not only the force F_t which is tangent to the airfoil chord line and F_n, which is normal to the chord line, but also the force along

and the moment about the spanwise coordinate axis. The spanwise force is neglected since it does not contribute to the torque produced by the blade element and contributes only slightly to the resultant force F_x. The pitching moment about the aerodynamic center of the airfoil is essentially zero, except at large angles of attack. In any event, the pitching moment on the blade element as it passes through the downstream portion of the streamtube is of opposite sign and of equal magnitude (within the limitations of this model). Therefore, it is of no consequence for calculation of rotor performance.

The two forces F_n and F_t, along with their resultant force F_x in the streamwise direction, are shown in figure 2. From this figure, it is seen that the resultant streamwise force F_x is given by:

$$F_x = - (F_n \sin\beta \sin\theta + F_t \cos\theta) \tag{5}$$

The forces F_t and F_n can be expressed in terms of the fluid density ρ, the plan area of the airfoil $\Delta h C \sin\beta$, where C is the airfoil chord length, and the relative velocity U_R of the fluid moving onto the airfoil

$$F_t = 1/2\ C_t\ \rho\ \frac{\Delta h c}{\sin\beta}\ U_R^2$$

$$F_n = -1/2\ C_n\ \rho\ \frac{\Delta h c}{\sin\beta}\ U_R^2 \tag{6}$$

In non-dimensional form, these forces can be written as:

$$F_t^+ = \frac{F_t \sin\beta}{1/2 \rho \Delta h C U_T^2} = C_t \left(\frac{U_R}{U_T}\right)^2$$

$$F_n^+ = \frac{-F_n \sin\beta}{1/2 \rho \Delta h C U_T^2} = C_n \left(\frac{U_R}{U_T}\right)^2 \tag{7}$$

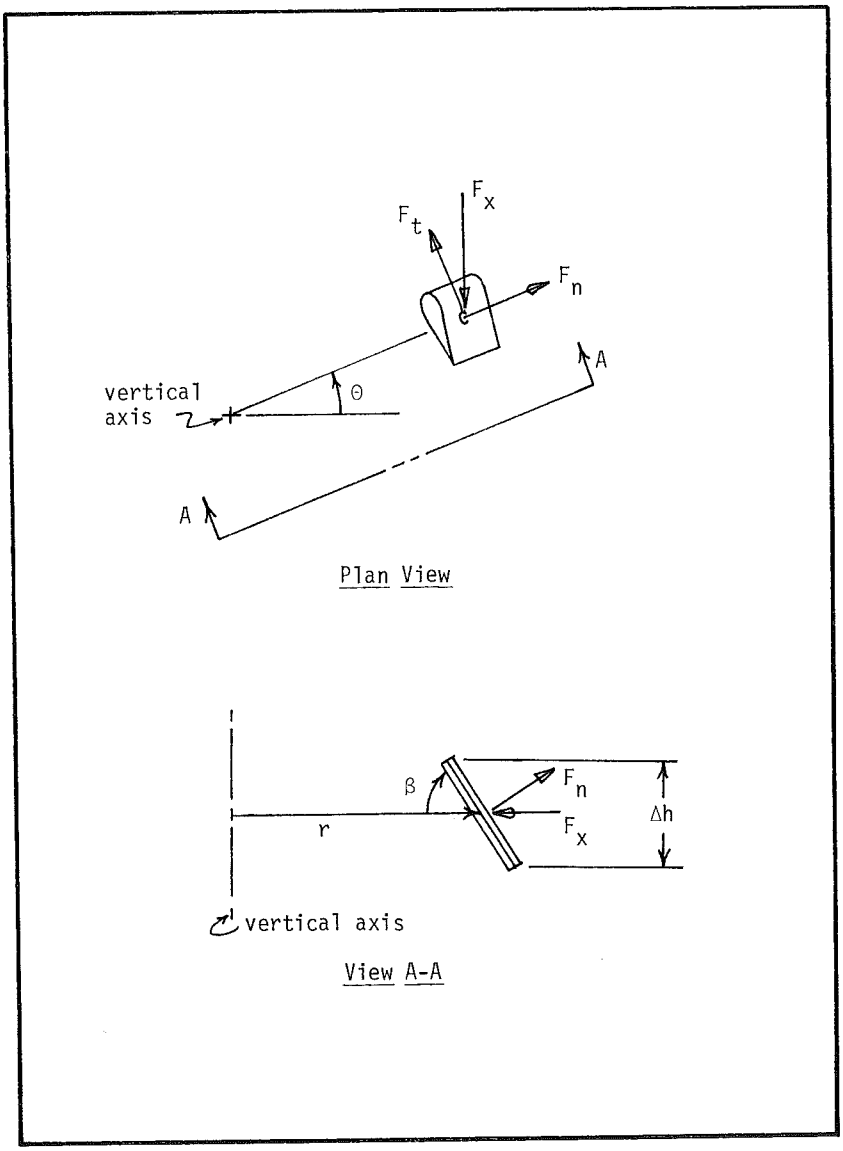

Figure 2 Blade Element Forces

where U_T is the maximum tip speed at the rotor equator.

The coefficients C_t and C_n are related to the more common airfoil lift and drag coefficients C_L and C_D by:

$$C_t = C_L \sin\alpha - C_D \cos\alpha$$
$$C_n = C_L \cos\alpha + C_D \sin\alpha \tag{8}$$

where α is the angle of attack between the airfoil chord line and U_R. Combining equations 4, 5, and 6, the non-dimensional streamwise force F_x^* can be written as:

$$F_x^* = \frac{NC}{4\pi r}\left(\frac{U_R}{U_\infty}\right)^2 \left(C_n - C_t \frac{\cos\theta}{\sin\theta\sin\beta}\right) \tag{9}$$

2.3 Relative Velocity Vector

The angle of attack and associated relative velocity in the plane of the airfoil cross section can be obtained from consideration of figure 3. The angle of attack α is given by:

$$\tan\alpha = \frac{U\sin\theta\sin\beta}{U\cos\theta + U_t} \tag{10}$$

where U_t is the tangential speed of the airfoil blade element. The relative velocity U_R in the plane of the airfoil cross section is obtained from the identity:

$$U_R \sin\alpha = U\sin\theta\sin\beta \tag{11}$$

2.4 Solution of the Momentum Equation

Defining an interference factor by:

$$a \equiv 1 - \frac{U}{U_\infty} \tag{12}$$

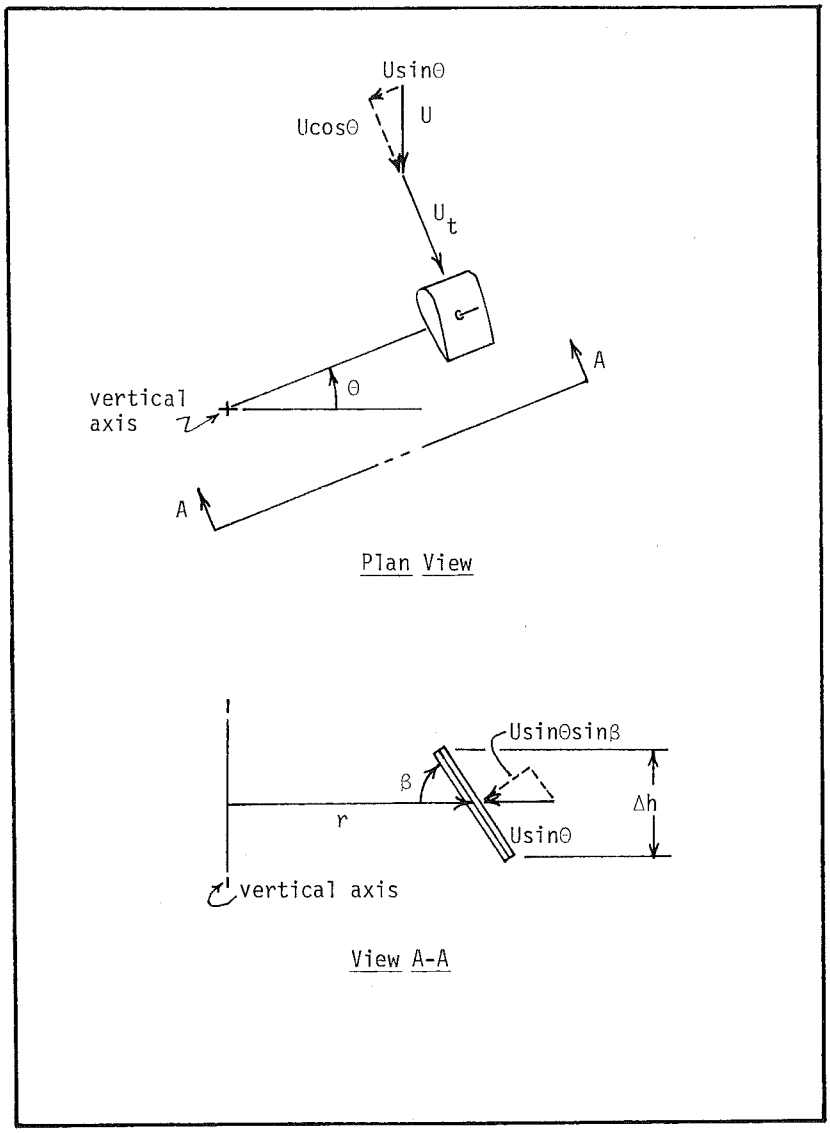

Figure 3 Relative Velocity Vector

and using this notation in conjunction with equations 3 and 4, the streamwise momentum equation can be written as:

$$a = F_x^* + a^2 \tag{13}$$

Equation 13 forms the basis for an iterative solution of the streamtube momentum equation. The function F_x^* is a rather complex function of "a" making an explicit solution for "a" all but impossible. The procedure for carrying out computations on a specified streamtube is as follows:

* "a" is set equal to zero which indicates that $U = U_\infty$.
* α is obtained from equation 10.
* C_n and C_t are obtained from airfoil data.
* U_R is obtained from equation 11.
* F_x^* is computed using equation 9.
* Using the present value of "a" and F_x^* in the right hand side of equation 13, a new value of "a" is computed.
* U/U_∞ is obtained from equation 12.
* The process is repeated starting with the calculation of α until the desired accuracy in "a" is obtained.

This process yields the value of U/U_∞ for the streamtube. Normally, convergence is rapid. For example, it has been found that computer (CDC 6600) processing time averages about 4×10^{-3} seconds per streamtube with a convergence error of less than 1.0×10^{-3} on "a".

2.5 Rotor Power Coefficient

Once the streamtube momentum equation has been solved, the torque produced by a rotor blade element as it passes through the streamtube can be obtained by:

$$T_s = 1/2\ \rho r C_t\ \frac{C\Delta h}{\sin\beta}\ U_R^2 \qquad (14)$$

In order to obtain the total torque on a blade for a particular value of θ, T_s must be integrated or summed over the number of blade segments N_s making up the blade. Each blade segment is assumed to be of a length $\Delta h/\sin\beta$ with T_s being calculated at the center of each element. The torque on a complete blade is thus given by:

$$T_B = \sum_{1}^{N_s} T_s \qquad (15)$$

To obtain the average torque produced on the rotor by all of the N blades, the value of T_B must be time averaged and multiplied by N. If values of T_s are obtained at N_t values of θ in increments of π/N_t, then the average rotor torque becomes:

$$\bar{T} = \frac{N}{N_t} \sum_{1}^{N_t} \sum_{1}^{N_s} T_s \qquad (16)$$

For all of the work presented herein, calculations were made at every 10° intervals in θ and at intervals in Z equal to one-tenth of the rotor height, where Z is measured from the rotor base along the vertical axis. Therefore, $N_s = 10$ and $N_t = 19$.

The rotor power coefficient in terms of the average rotor torque is given by:

$$C_p = \frac{T\omega}{1/2\rho \sum_{1}^{N_s} 2r\Delta h U_\infty^3} \qquad (17)$$

where ω is the angular speed of the rotor. Combining equations 14, 15, 16 and 17, one obtains:

$$C_p = \frac{\sum_{1}^{N_s} \sum_{1}^{N_t} \left[\frac{NC}{2R\sin\beta} \frac{U_t}{U_\infty} \left(\frac{U_R}{U_\infty}\right)^2 C_t \right]}{N_t \sum_{1}^{N_s} \frac{r}{R}} \tag{18}$$

where R is the equatorial radius of the rotor. For convenience, the quantity in brackets is denoted by C_{pl}, which can be thought of as a local power coefficient based on the local torque and the area $2R\Delta h$. Therefore:

$$C_p = \frac{\sum_{1}^{N_s} \sum_{1}^{N_t} C_{pl}}{N_t \sum_{1}^{N_s} \frac{r}{R}} \tag{19}$$

3.0 Discussion of Results

In order to test the accuracy of the DART model, predictions were made for two rotor configurations which were recently tested by Sandia Labs in the LTV wind tunnel. Comparisons were then made between the DART model and the single streamtube model using exactly the same airfoil data. The DART model was then used to predict solidity and Reynold's number effects for rotors with constant chord blades, height to diameter ratios equal to 1.0, and uniform free stream velocities. Finally, the contribution of various blade segments to the overall power output and the effects of wind shear were investigated briefly.

3.1 Comparison with Test Results

Wind tunnel tests of two 2-meter diameter Darrieus rotors were conducted in the LTV wind tunnel in May, 1975. These tests will be documented in an upcoming report. Both a two bladed rotor with a value of NC/R = 0.18 and a three bladed rotor with a value of NC/R = 0.27 were tested. The aluminum rotor blades were NACA 0012 airfoils. The tests were conducted with freestream velocities of 7, 9, and 11 meters per second. For the 9 meter per second windspeed, blade Reynold's numbers on the rotor tip range from about 0.10×10^6 to 0.36×10^6 for tip to wind speed ratios of 2 and 7 respectively. Data to be used in the DART model were selected from reference [7] for the NACA airfoil for a blade Reynold's number of 0.30×10^6 (data is unavailable for Reynold's numbers as low as 0.10×10^6). The drag coefficient at zero angle of attack was also obtained from reference [7] at the test Reynold's number instead of the "effective Reynold's number." The effective Reynold's number is normally used to predict performance under freeflight conditions and attempts to eliminate the effect of wind tunnel turbulence. For large angles of attack, greater than about 30°, the data in reference [8] was used. Values of C_n and C_t are given in table 1 for a blade Reynold's number of 0.3×10^6 as well as for 3.0×10^6.

Figure 4 shows the relatively good agreement between wind tunnel measurement of the rotor power coefficient and the DART model predictions using data for a blade Reynold's number of 0.3×10^6. The failure to agree exactly on the left hand portion of the curves is at least partially due to the difference in blade Reynold's numbers between test and analysis. The DART prediction of C_p would be expected to be higher in this region

TABLE OF DATA

RE= .30E+06
CDO=.0085

ALPHA	CN	CT+CDO
0.0	0.000	0.0000
2.0	.200	.0061
5.0	.499	.0393
7.5	.765	.0910
10.9	.850	.1230
11.0	.860	.0810
15.0	.834	.0560
17.5	.821	.0230
21.0	.815	-.0300
30.0	1.160	-.0500
40.0	1.500	-.0500
50.0	1.750	-.0300
60.0	1.950	-.0100
70.0	2.050	.0100
80.0	2.080	.0500
90.0	2.060	.0900
100.0	2.040	.1250
110.0	1.950	.1500
120.0	1.850	.1500
130.0	1.700	.1500
140.0	1.500	.1500
150.0	1.170	.1400
154.0	1.000	.1250
160.0	.780	.1000
164.0	.720	.0600
168.0	.740	.0450
170.0	.760	.0400
172.0	.850	.0250
175.0	.500	.0250
180.0	0.000	.0250

RE= .30E+07
CDO=.0081

ALPHA	CN	CT+CDO
0.0	0.000	0.0000
2.0	.200	.0066
5.0	.498	.0421
10.0	.987	.1670
15.0	1.396	.3560
17.5	1.497	.4320
18.0	1.326	.1890
20.0	1.136	.0940
25.0	1.042	-.0110
30.0	1.160	-.0500
40.0	1.500	-.0500
50.0	1.750	-.0300
60.0	1.950	-.0100
70.0	2.050	.0100
80.0	2.080	.0500
90.0	2.060	.0900
100.0	2.040	.1250
110.0	1.950	.1500
120.0	1.850	.1500
130.0	1.700	.1500
140.0	1.500	.1500
150.0	1.170	.1400
154.0	1.000	.1250
160.0	.780	.1000
164.0	.720	.0600
168.0	.740	.0450
170.0	.760	.0400
172.0	.850	.0250
175.0	.500	.0250
180.0	0.000	.0250

Table 1. Airfoil Data

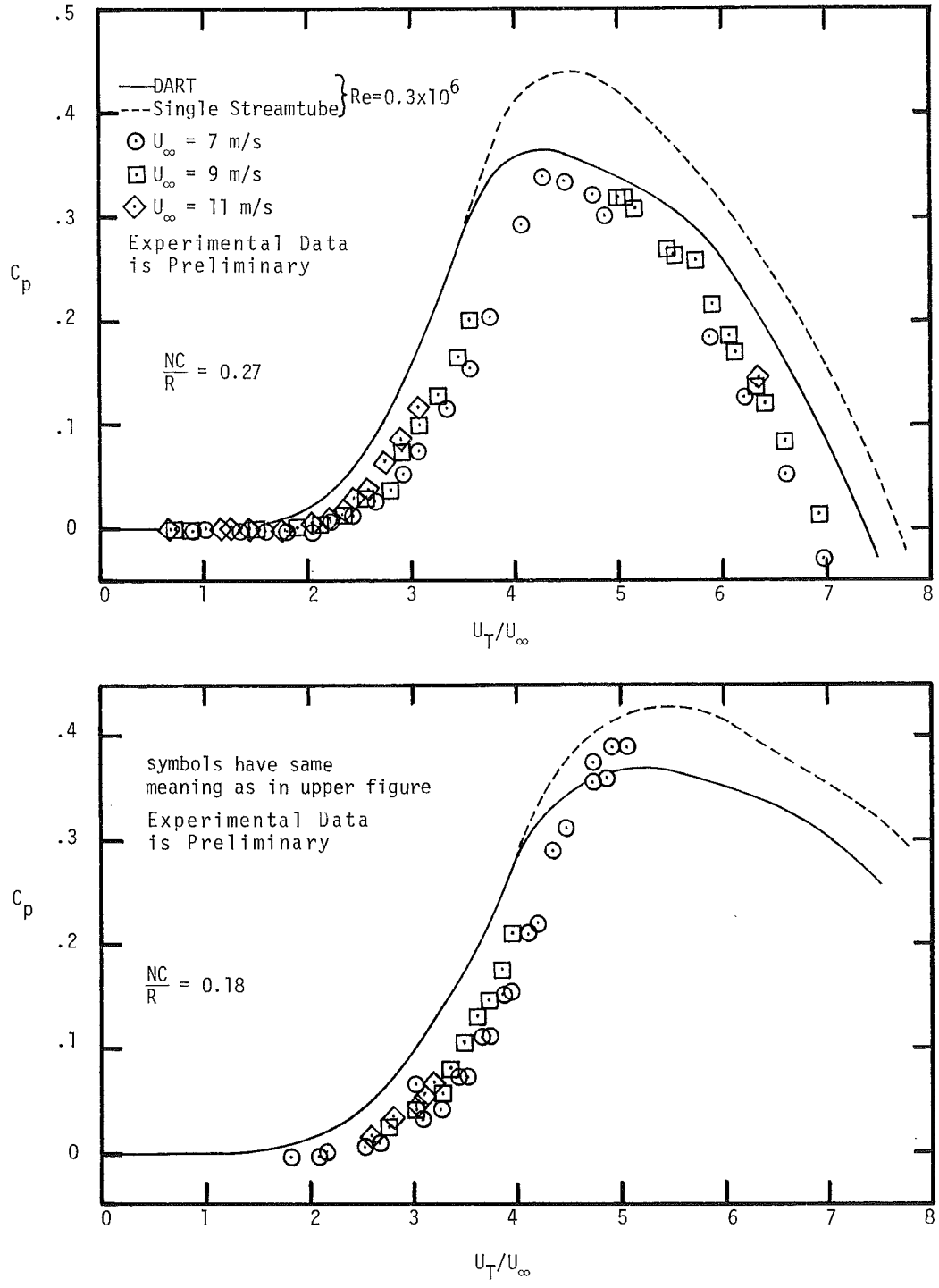

Figure 4 Comparison of DART and Single Streamtube Models with Sandia Test Data (Zm dia. rotor)

since increasing the blade Reynold's number tends to delay aerodynamic stall. Unfortunately, airfoil data is not available at the low Reynold's numbers, consistent with the test Reynold's numbers, on the left hand side of the C_p curve. On the right hand side of the curve, the test Reynold's numbers at the rotor tip and the Reynold's numbers used in the DART analysis are nearly the same. The DART prediction is again somewhat high which may be in part due to blade Reynold's numbers toward the rotor hub which are again less than that used in the analysis.

3.2 Comparison with Single Streamtube Model

Also shown in figure 4 is a comparison between C_p predicted by the DART model and the single streamtube model. As is typical, agreement between the models is quite good at low tip to wind speed ratios. This is due to the fact that for lightly loaded blades (i.e. low tip to wind speed ratios or low solidities) the distribution of rotor streamtube velocities is reasonably uniform and is almost equal to the freestream velocity. For highly loaded blades, on the other hand, the distribution of rotor streamtube velocities is extremely non-uniform and the uniform rotor velocity approximation is invalid. Figure 5 depicts an example of the variation of streamtube velocities through the rotor with a solidity of 0.3 operating at a tip to wind speed ratio of 3.5 and a blade Reynold's number of 0.3×10^6. The single streamtube model predicts a uniform value of rotor wind speed to freestream velocity of 0.756.

3.3 Solidity and Reynold's Number Effects

Figures 6 and 7 depict the effect of solidity at blade Reynold's numbers of 0.3×10^6 and 3.0×10^6. In figure 8 several quantities which

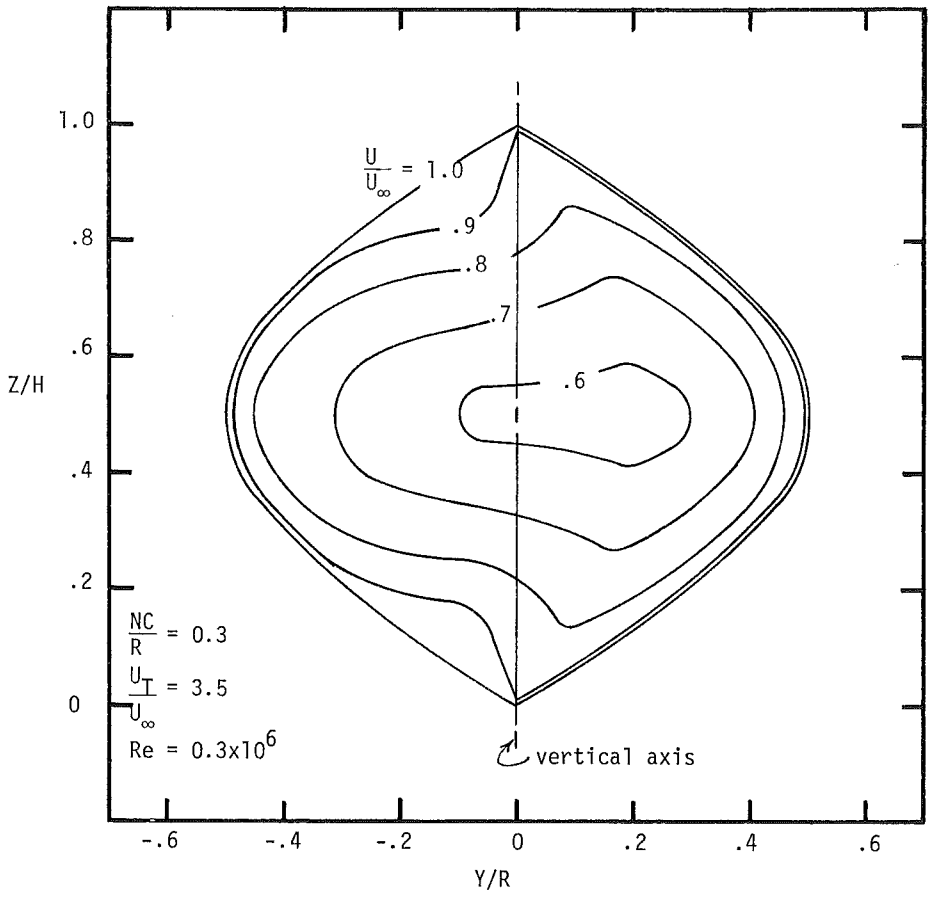

Figure 5 Variation of Streamtube Velocities Through the Rotor (view looking upstream through the rotor)

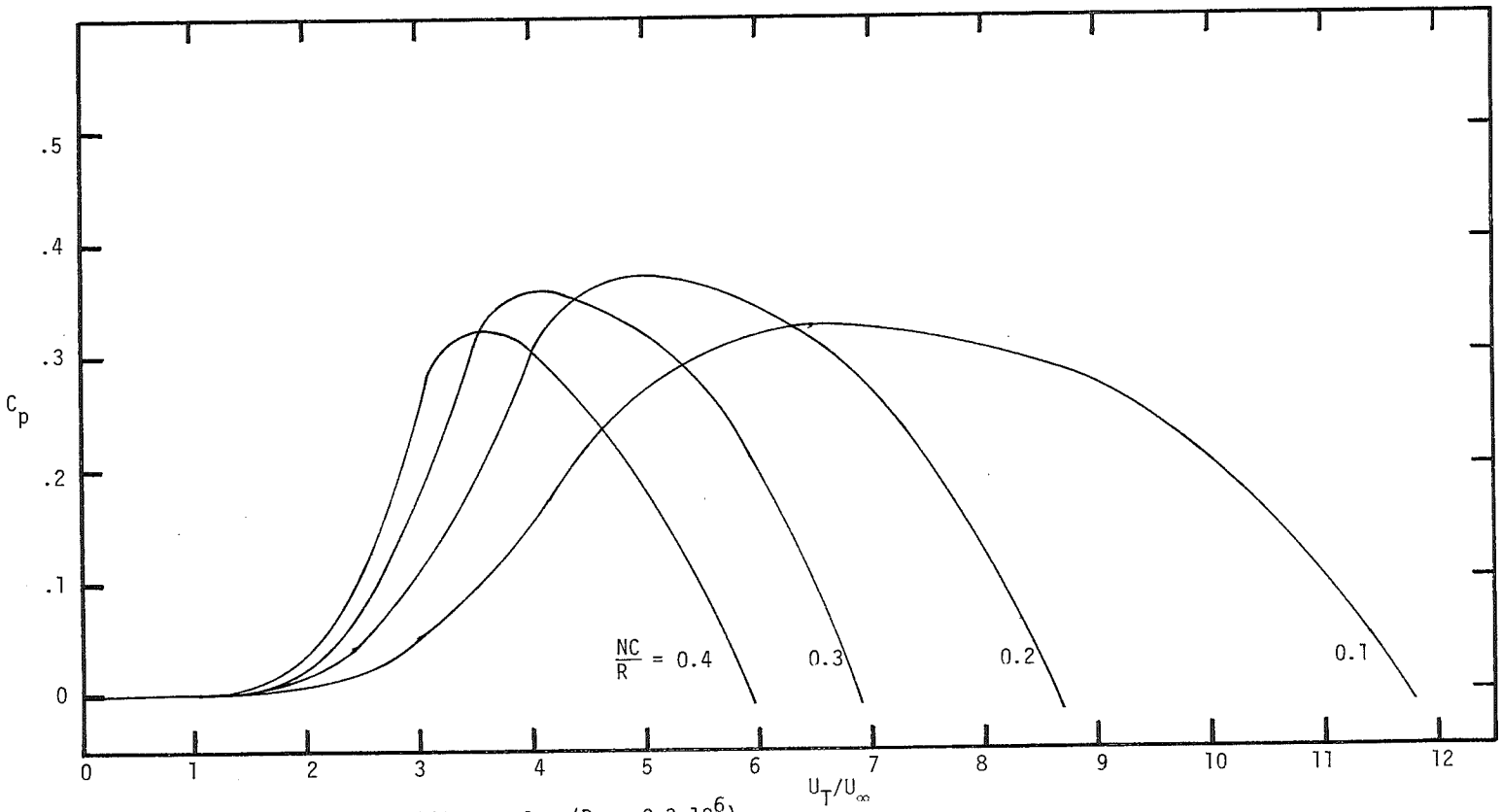

Figure 6 The Effect of Solidity on C_p (Re = 0.3×10^6)

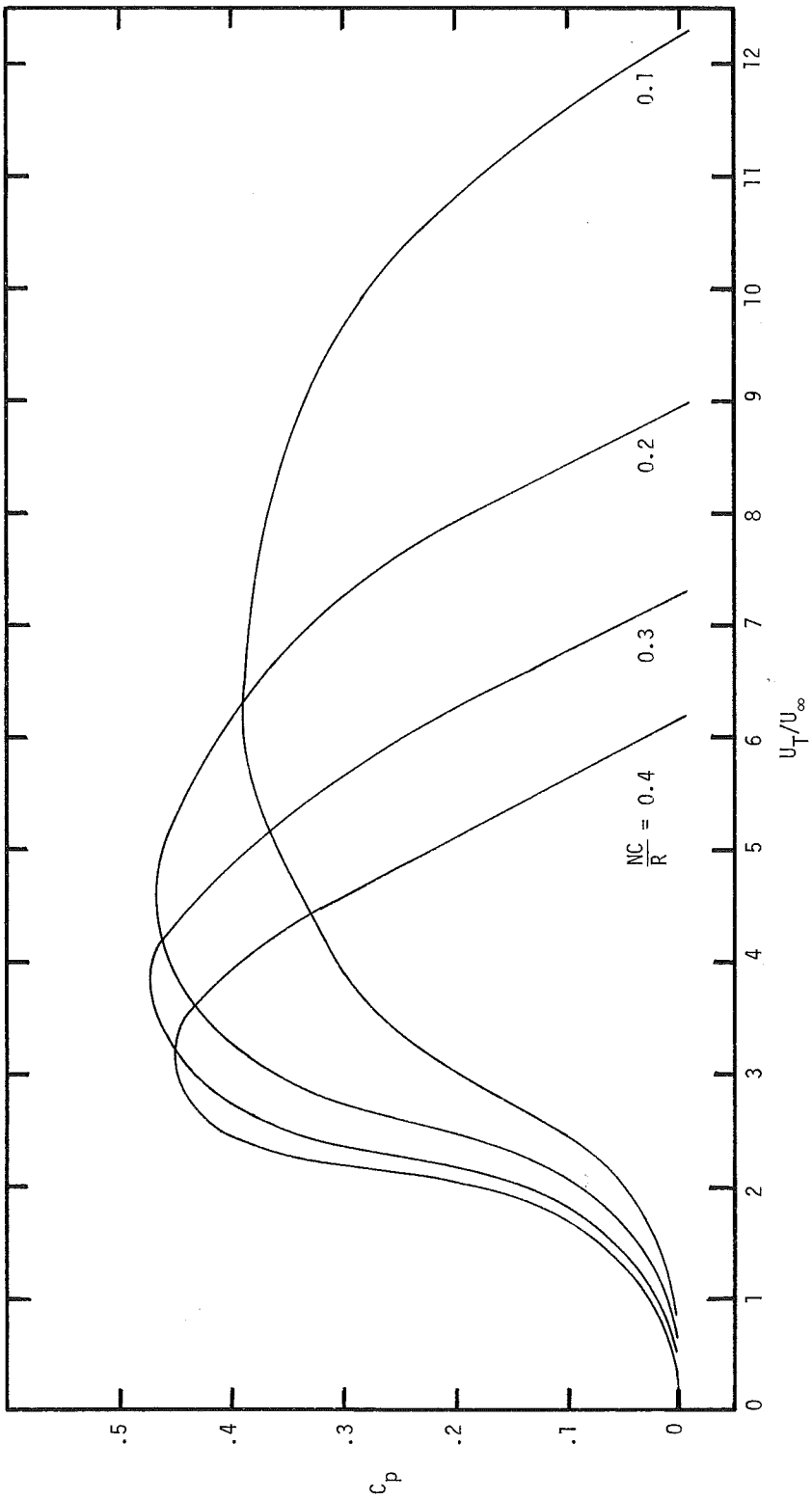

Figure 7 The Effect of Solidity on C_p (Re = 3.0×10^6)

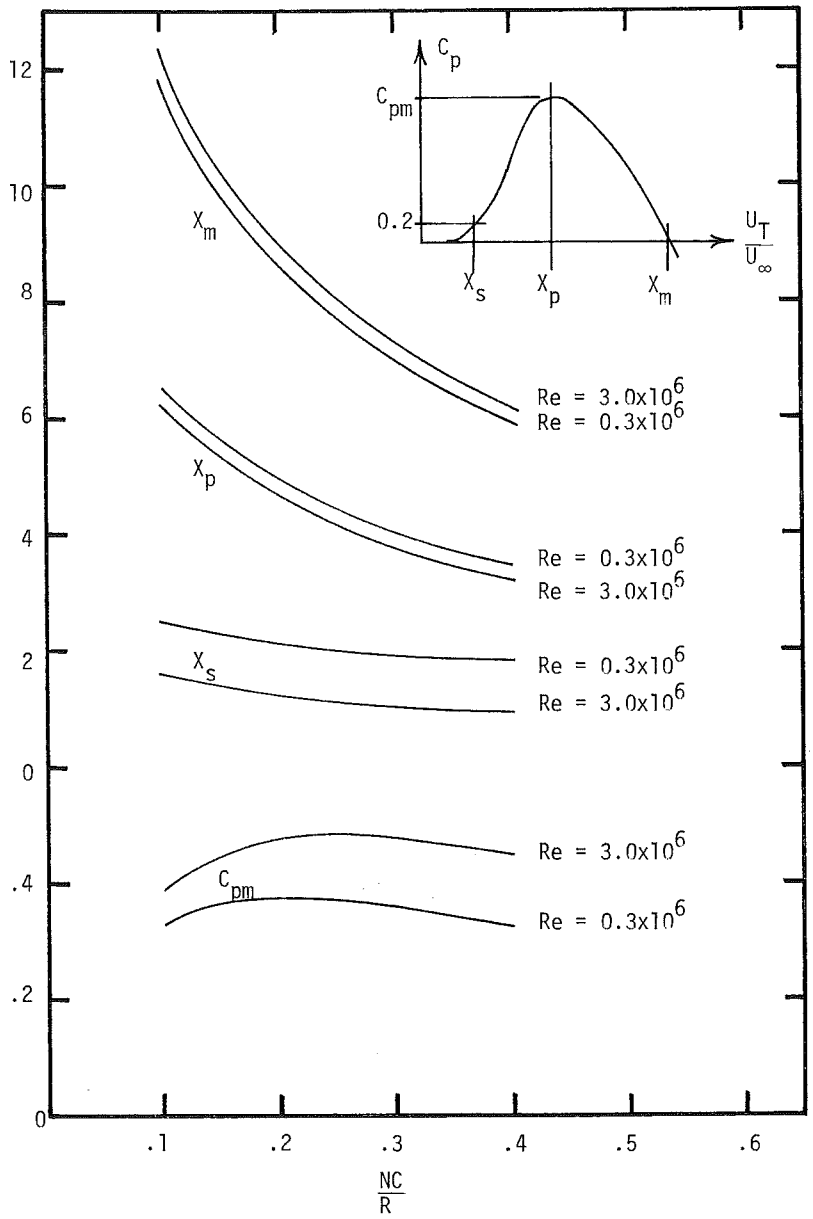

Figure 8 C_p Curve Characterization

characterize the C_p curve are given as a function of solidity and Reynold's number. It is somewhat interesting to note that two correlations can be obtained from examination of figure 7. The first of these is that:

$$X_p = (X_m + X_s)/2.22 \tag{20}$$

The second is that X_s and X_m vary with solidity according to equations of the form:

$$X^{-1} \sim C_1 + \frac{NC}{R} \tag{21}$$

where C_1 is some function of the Reynold's number. The variation of X_m with Reynold's number is dominated by the skin fiction drag coefficient. On the other hand, variation of X_s with Reynold's number is dominated by profile drag due to aerodynamic stall.

3.4 Blade Power Distribution

To provide an example of the contribution that various blade elements make to the overall power coefficient a rotor with a solidity of 0.3 operating at a Reynold's number of 3×10^6 was examined. The results are plotted in figure 9 and depict the contribution of the blades extending over various vertical heights about the equator. For this particular example the central 60% of the rotor produces about 84% of the total power output for a tip to wind speed ratio of 4. It is interesting to note, however, that as the tip to wind speed ratio approaches 7 that the central 60% of the rotor is producing drag on the rotor and is in fact being driven by the outer 40%.

3.5 Wind Shear Effects

In order to evaluate the sensitivity of the Darrieus turbine to

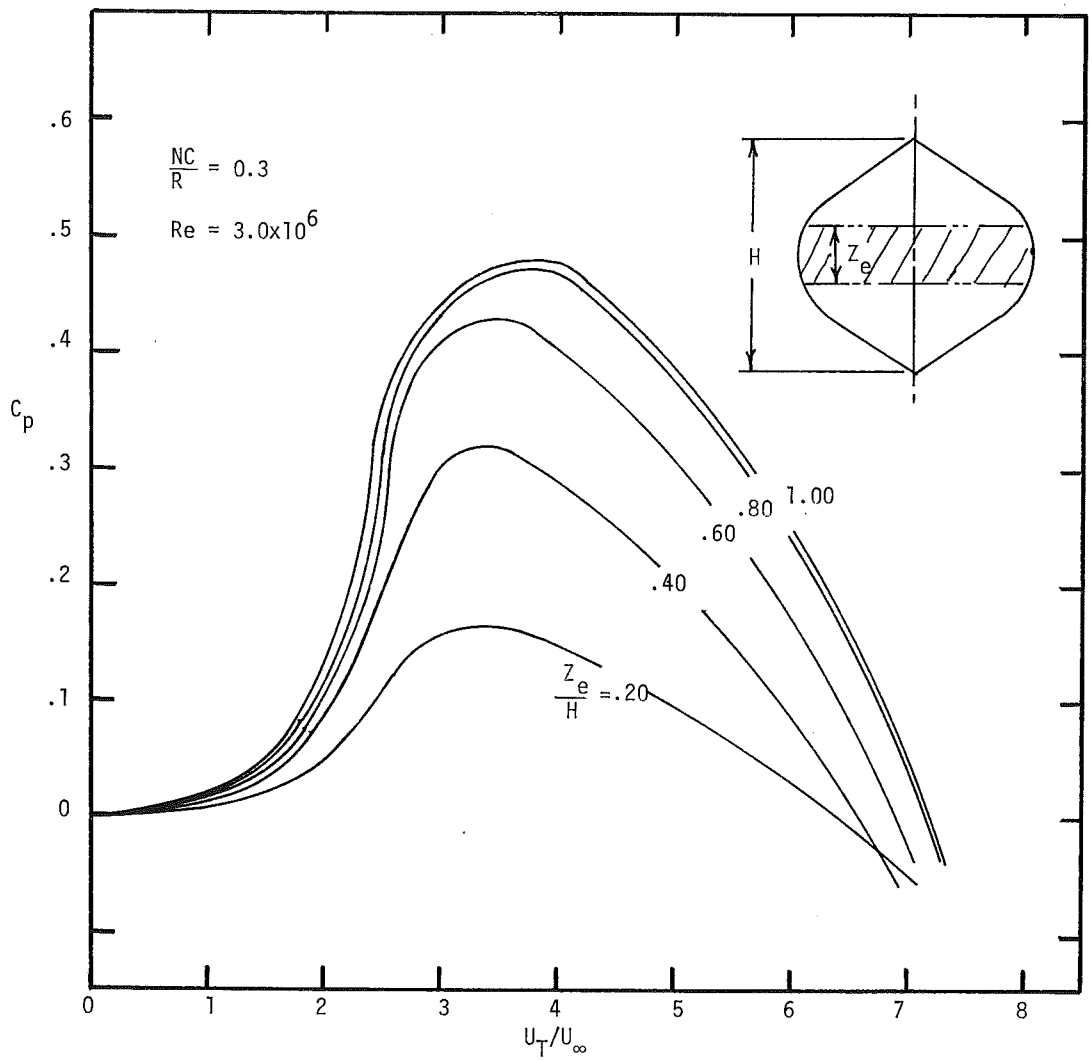

Figure 9 Contribution of Equatorial Band to C_p

atmospheric wind shear the common 1/7 power freestream velocity profile was used [9-10]. The bottom of the rotor was assumed to be at ground level resulting in the following relationship.

$$\frac{U_\infty}{U_{\infty C}} = \left(\frac{2Z}{H}\right)^{1/7} \tag{22}$$

where $U_{\infty C}$ is the freestream velocity upstream of the center or equator of the rotor. The quantity Z/H is the ratio of the height above the base of the rotor to the overall rotor height.

Figure 10 shows a comparison between power coefficient curves for a rotor with and without wind shear present.

The difference between the two curves is small when the centerline or equatorial freestream velocity at Z/H = 0.5 is used as the basis for computing C_p and U_T/U_∞. If, however, the freestream velocity at a height of Z/H = 0.45 is used, the C_p curves with and without wind shear are virtually identical.

4.0 DART Computer Model

While no attempt will be made to discuss the program in detail, the general features of the input - output characteristics will be given along with a listing of the DART program.

4.1 Input

The turbine configuration is input in terms of the blade solidity NC/R and the turbine height to radius ratio H/R. The blade shape is that of a sine curve which closely approximates a troposkein.

Airfoil section data is input in tabular form in terms of C_n and C_t for various values of the angle of attack α. The drag coefficient

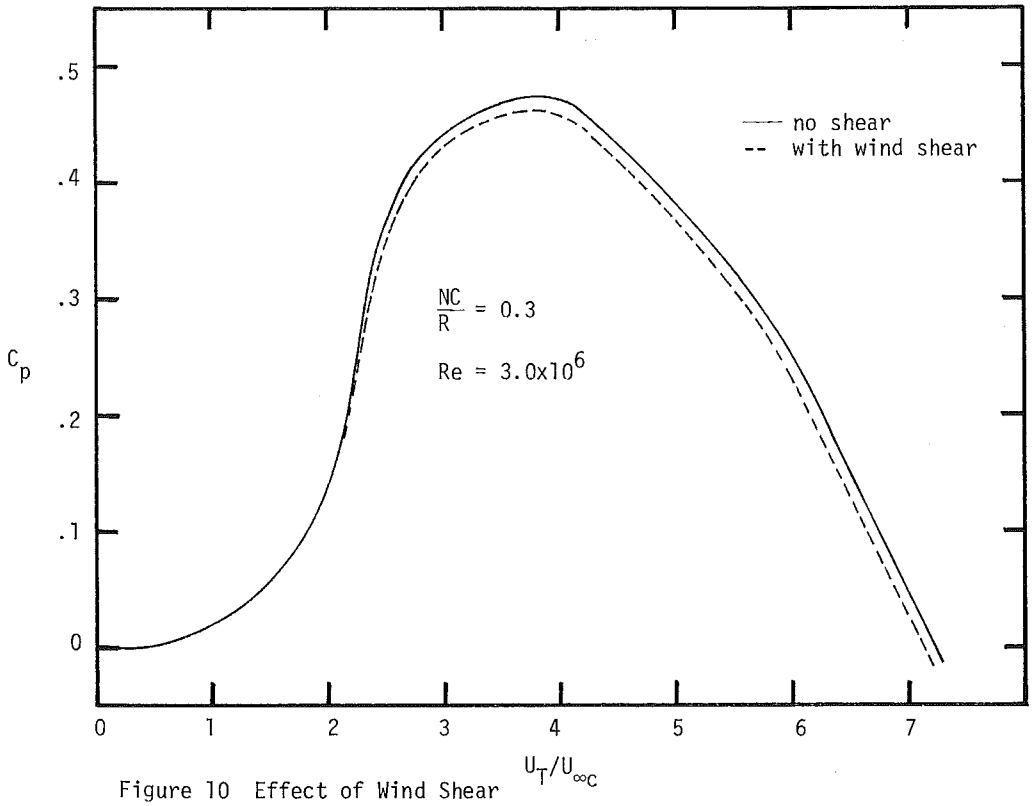

Figure 10 Effect of Wind Shear on Rotor Performance

C_{DO} at zero angle of attack is also specified. C_{DO} is subtracted from the tabulated value of C_t to obtain the actual value of C_t used for computational purposes. Thus, when tabulating C_t, this somewhat anamolous though conventional procedure of separating out C_{DO} must be considered. A choice of tip to wind speed ratios for which calculations are to be made can be obtained by specifying the number of ratios to be examined, the lowest value, and the increment between values. Finally the choice of a uniform freestream velocity or a 1/7 power profile is made available. Input data code names are given in Table 2.

4.2 Output

The output is tabulated for each streamtube for which calculations are made. The streamtube position is identified by the angle θ in degrees and the vertical distance from the rotor base which is characterized by Z/H. The blade element angle of attack α in radians and the non-dimensional forces F_t^+ and F_n^+, which are defined by equation 7, are next tabulated. The ratio of local streamtube velocity to freestream velocity U/U_∞ is given next and is based upon the appropriate value of U_∞ for the given value of Z/H. In the next two columns the local power coefficient, as defined by equations 18 and 19 along with its summation are given. At the conclusion of each tabular set of data, as indicated above, the overall value of C_p is given along with the corresponding rotor tip to wind speed ratio.

function	code name	quantity
rotor geometry	S	NC/R (solidity)
	HR	H/R
airfoil data	XCDO	C_{DO}
	TA	tabular value of α in degrees
	TCN	tabular value of C_n
	TCT	tabular value of C_t
	NTBL	number of tabular values
tip to wind speed selection	NTSR	number of turbine speed ratios
	TSRI	initial turbine speed ratio
	DTSR	difference in turbine speed ratios
wind shear	SHEAR	SHEAR = 0. , U_∞ = const. SHEAR = 1. , $U_\infty \sim Z^{1/7}$

Table 2. DART Input Code

```
PROGRAM      DART                                    CDC 6600 FTN V3.0-V34A OPT=1

                  PROGRAM DART(INPUT,OUTPUT)
                  COMMON/TABLS/TA(50),TCN(50),TCT(50),NTBL1,XCDO
                  SHEAR=0.
                  NT=19
 5                ERR=.001
                  PY=4.*ATAN(1.)
                  DTR=PY/180.
                  READ 1,XCDO
                1 FORMAT(6F10.0)
10                PRINT 19,XCDO
               19 FORMAT(30X,4E14.6)
                  READ 20,NTBL
               20 FORMAT(I2)
                  NTBL1=NTBL-1
15                DO 21 I=1,NTBL
                  READ 1, TA(I),TCN(I),TCT(I)
               21 PRINT 22, I,TA(I),TCN(I),TCT(I)
               22 FORMAT(5X,I2,2X,3E14.6)
                  READ 3,NTSR,TSRI,DTSR
20              3 FORMAT(I10,2F10.0)
            C     HR = H/R
            C     S = NC/R
                  READ 1, HR,S
                  PRINT 140, S,HR
25            140 FORMAT(1X,*S=*,E8.2,*H/R=*,E8.2)
                  DO 60 J=1,NTSR
                  PRINT 5
                5 FORMAT(6X,*THETA*,8X,*Z/H*,10X,*ALPHA*,8X,*FNPLUS*,7X,
                 1*FTPLUS*,7X,*U/UINF*,7X,*CPLOC*,8X,*CPSUM*)
30          C     X=UTMAX/UINFCENTER
                  X=TSRI+(J-1.)*DTSR
                  IF(SHEAR.EQ.1.) GO TO 6
                  NZH=5
                  GO TO 7
35                6 NZH=10
                  7 CPSUM=0.
                  RRSUM=0.
                  DO 90 I=1,NZH
                  IF(SHEAR.EQ.1.) GO TO 8
40          C     ZH = Z/H
                  ZH=(2.*I-1.)/(4.*NZH)
            C     U1 = UTMAX/UINF
                  U1=X
                  GO TO 9
45                8 ZH=(2.*I-1.)/(2.*NZH)
                  U1=X/((2.*ZH)**(1./7.))
                  9 CONTINUE
            C     RR = RLOCAL/RMAX
                  RR=SIN(PY*ZH)
50                RRSUM=RRSUM+RR
                  BETA=ATAN(HR/(PY*COS(PY*ZH)))
                  SBETA=SIN(BETA)
                  DO 89 K=1,NT
            C     T = THETA IN DEGREES
55                T=90.*(2.*K-1.)/NT
```

```
PROGRAM      DART

                  THETA=T*DTR
                  STH=SIN(THETA)
                  CTH=COS(THETA)
            C     AA = INTERFERENCE FACTOR
60                AA=0.
                  NTRY=0
            C     U2 = U/UINF
          100 U2=1.-AA
            C     U3 = UT/U
65                U3=RR*U1/U2
                  ALPHA=ATAN(STH*SBETA/(CTH+U3))
                  IF(ALPHA.LT.0.) ALPHA=PY+ALPHA
                  SAL=SIN(ALPHA)
                  ALD=ALPHA/DTR
70                CALL CNCT(ALD,CN,CT)
            C     U4 = UR/U
                  U4=STH*SBETA/SAL
            C     U5 = (UR/UINF)**2
                  U5=(U4*U2)**2
75                FX=S*U5*(CN-CT*CTH/(STH*SBETA))/(4.*PY*RR)
                  ANEW=AA*AA+FX
                  NTRY=NTRY+1
                  IF(NTRY.LE.100) GO TO 81
                  U2=-U2
80                GO TO 130
           81     IF(ANEW.GT.1.) GO TO 70
                  IF(ABS(ANEW-AA).LT.ERR) GO TO 130
                  AA=ANEW
                  GO TO 100
85           70   U2=0.
          130     CPLOC=(CT*S*X*RR*(X*U2*U4/U1)**2)/(2.*SBETA)
                  CPSUM=CPSUM+CPLOC
                  FN=-CN*U5/(U1**2)
                  FT=-CT*FN/CN
90                PRINT 80,T,ZH,ALPHA,FN,FT,U2,CPLOC,CPSUM
           89     CONTINUE
           80     FORMAT(1X,8E13.4)
           90     CONTINUE
                  CP=CPSUM/(NT*RRSUM)
95                PRINT 30,CP,X
           30     FORMAT(1X,*CP=*,E14.6,*UTMAX/UINFCENTER=*,E14.6)
           60     CONTINUE
                  END

SUBROUTINE   CNCT

                  SUBROUTINE CNCT(A,CN,CT)
                  COMMON/TABLS/TA(50),TCN(50),TCT(50),NTBL1,XCDO
                  DO 1 I=1,NTBL1
                  J=I
 5                IF(A.GE.TA(I) .AND. A.LE.TA(I+1)) GO TO 2
                1 CONTINUE
                2 X=(A-TA(J))/(TA(J+1)-TA(J))
                  CN=TCN(J)+X*(TCN(J+1)-TCN(J))
                  CT=TCT(J)+X*(TCT(J+1)-TCT(J))
10                IF(A.LE.15.) CT=CT-XCDO
                  RETURN
                  END
```

5.0 Conclusions and Recommendations

In conclusion, the multiple streamtube model appears to be a substantial improvement over the single streamtube model in that: it more precisely predicts measured values of C_p, it more precisely predicts distributed effects such as blade forces and rotor wake velocity distributions, and it is adaptable to inclusion of spatial variations in free-stream velocity. On the other hand, the model is inadequate in describing many of the details of the flow field such as are related to streamtube distortions and interactions. The most serious deficiency is that, under conditions of large solidity and high tip to wind speed ratios, the simple momentum considerations inherent in the model break down. This deficiency is also suffered by the single streamtube model.

In considering recommendations for further study, the work can be categorized according to the magnitude of modification necessary to the present model. The first category involves work which can be conducted with the present DART model without any modifications. The second category involves work which can be conducted with modifications in input information with little change to the basic model. The third category involves reasonably major changes in the model.

The present DART model should be used to make investigations concerning blade aerodynamic force distributions for examination of rotor structural and vibration problems. In addition, these blade force distributions can be used to assess the transient behavior of a rotor during a single period of revolution. A more extensive investigation of the effects of windshear, including vertical distributions different from the 1/7 power profile as well as horizontal distributions, should be

undertaken. A study using symmetrical airfoil data other than that for the NACA 0012 should be undertaken to investigate the effect on C_p.

With regard to the second category, which requires minor modifications to the DART program, a systematic study of the effects of blade taper or non-uniform blade chord distributions should be made. An investigation of the effects of various spanwise blade shapes should also be made in conjunction with both straight and tapered blade chord distributions. An attempt to use the local blade element Reynold's number in the calculations should be made. This will undoubtedly require not only interpolation between Reynold's numbers where airfoil data exists, but also extrapolation of such data in some cases. The potential of non-symmetrical airfoils should be examined. This will require some minor modification of the DART program to accommodate such input since calculations will be required over the range θ = 0 to 360° instead of the present range of 0 to 180° for symmetrical airfoils.

Investigations which would require more extensive modification of the DART model might include; the inclusion of most wake effects, the modification of the momentum equation for cases when it breaks down, and inclusion of some of the effects of streamtube distortion and interaction.

Bibliography

1. Blackwell, B. F. and Feltz, L. V. "Wind Energy - A Revitalized Pursuit," Sandia Laboratory Report SAND75-0166, March (1975).

2. Banas, J. F., Kadlec, E. G., Sullivan, W. N. "Methods for Performance Evaluation of Synchronous Power Systems Utilizing the Darrieus Vertical-Axis Wind Turbine," Sandia Laboratory Report SAND75-0204, April (1975).

3. Wilson, R. E., Lissamon, P. B. S., Applied Aerodynamics of Wind Power Machines, Oregon State University, May 1974.

4. South, P. and Rangi, R. "Preliminary Tests of a High Speed Vertical Axis Windmill Model," National Aeronautical Establishment of Canada Report LTR-LA-74, March (1974).

5. Templin, R. J. "Aerodynamic Performance Theory for the NRC Vertical-Axis Wind Turbine," National Research Council of Canada Report LTR-LA-160, June (1974).

6. Glauert, H. The Elements of Aerofoil and Airscrew Theory, The Macmillan Co., New York, (1943).

7. Jacobs, E. N. and Sherman, A. "Airfoil Section Characteristics as Affected by Variations of the Reynold's Number," NACA Report No586, 23rd Annual NACA Reports 577-611, (1937).

8. Riegels, F. W. Aerofoil Sections, Translated from German by D. G. Randell, Butterworths, London, (1961).

9. Davenport, A. G. "The Dependence of Wind Loads on Meteorological Parameters," Proc. Wind Effects on Buildings and Structures Conference, International Research Seminar, University of Toronto Press, (1968).

10. Reed, J. W., Maydew, R. C., and Blackwell, B. F. "Wind Energy Potential in New Mexico," Sandia Laboratory Report SAND74-0071, July (1974).

Distribution:

R. J. Templin
Low Speed Aerodynamics Section
NRC-National Aeronautical
Establishment
Ottawa 7, Ontario, CANADA K1A0R6

A. Robb
Memorial University of Newfoundland
Faculty of Engineering and Applied
Sciences
St. John's Newfoundland
CANADA A1C 5S7

H. Sevier
Rocket and Space Division
Bristol Aerospace Ltd.
PO Box 874
Winnipeg, Manitoba
R3C 2S4 CANADA

V. A. L. Chasteau
Department of Mechanical Engineering
The University of Auckland
Private Bag
Auckland, NEW ZEALAND

G. Herrera
Jet Propulsion Lab
4800 Oak Grove Drive
Pasadena, CA 91103

NASA Langely Research Center
Hampton, VA 23365
Attn: R. Muraca, MS 317

NASA Lewis Research Center
21000 Brookpark Road
Cleveland, Oh 44135
Attn: J. Savino, MS 500-201
R. Thomas

ERDA (2)
1800 G. Street NW
Washington, D.C. 20550
Attn: L. V. Divone
B. F. Blackwell

B. Vance
Science Applications
1200 Prospect Street
La Jolla, CA 92073

A. N. L. Chiu
Wind Engineering Research
Digest
Spalding Hall 357
University of Hawaii
Honolulu, HI 96822

R. N. Meroney
Colorado State University
Dept. of Civil Engineering
Fort Collins, CO 80521

Chumin Fu
Illinois Institute of
Technology
Department of Physics
Chicago, IL 60616

New Mexico State University (3)
PO Box 3450
Las Cruces, NM 88003
Attn: H. A. Daw
M. M. Sluyter
R. L. San Martin

Oklahoma State University (2)
Stillwater, OK 74074
Attn: W. L. Hughes,
EE Department
D. K. McLaughlin,
ME Department

Oregon State University
Corvallis, OR 97331
Attn: R. Wilson,
ME Department

Texas Tech University
Lubbock, TX 79409
Attn: K. C. Mehta, (1)
CE Department
J. Strickland, (20)
ME Department

R. G. Watts
Tulane University
Department of Mechanical
Engineering
New Orleans, LA 70118

Distribution (Continued):

University of New Mexico (2)
Albuquerque, NM 87131
Attn: K. T. Feldman,
Energy Research Center
V. Skoglund,
ME Department

Nevada Operations Office, ERDA (2)
PO Box 14100
Las Vegas, NV 89114
Attn: R. Ray, Operations
H. Mueller, ARL

Los Alamos Scientific Lab (6)
PO Box 1663
Los Alamos, NM 87544
Attn: R. R. Brownlee, J-9
J. R. Bartlit, Q-26
J. D. Balcomb, Q-DO-T
R. G. Wagner, P-5
J. Nachamkin, T-DO-TEC
S. W. Depp, E-DO

ERDA/ALO (3)
Kirtland AFB East
Albuquerque, NM 87115
Attn: D. C. Graves

R. Camarero
Faculty of Applied Science
University of Sherbrooke
Sherbrooke, Quebec
CANADA J1K 2R1

American Wind Energy Association
21243 Grand River
Detroit, MI 48219

Captain M. E. Dewitte (2)
AFWL/DEZ
Kirtland Air Force Base
Albuquerque, NM 87117

E. E. Anderson
Department of Mechanical
Engineering
South Dakota School of Mines
and Technology
Rapid City, SD 57701

M. Snyder
Aero Engineering Department
Wichita State University
Wichita, KS 67208

R. A. Parmelee
Department of Civil Engineering
Northwestern University
Evanston, IL 60201

Ralph Beckman
Research and Design Institute
PO Box 307
Providence, RI 02901

Binx Selby
5595 E. Arapaho
Boulder, CO 80302

J. Park
Helion
PO Box 4301
Sylmar, CA 91432

W. F. Foshag
Aerophysics Company
3500 Connecticut Av. NW
Washington, D.C. 20008

W. L. Harris
Aero/Astro Department
MIT
Cambridge, MA 02139

K. Bergey
Aero Engineering Department
University of Oklahoma
Norman, OK 73069

J. Fischer
F. L. Smidth & Company A/S
Vigerslevalle 77
2500 Valby
DENMARK

O. Krauss
Division of Engineering
Research
Michigan State University
East Lansing, MI 48823

Distribution (Continued):

A. H. Stodhart
Electrical Research Associates
Cleeve Road
Surrey, ENGLAND

V. Nelson
Department of Physics
West Texas State University
PO Box 248
Canyon, TX 79016

E. Gilmore
Amarillo College
Amarillo, TX

R. K. Swanson
Southwest Research Institute
San Antonio, TX

L. Llilidahl
Building 303
Agriculture Research Center
USDA
Beltsville, MD 20705

D. Grimmer, Q-24
Mail Stop 571
Los Alamos Scientific Laboratory
Los Alamos, NM 87545

C. H. Dunn
Prof. of Electrical Engineering
Wichita State University
Wichita, KS 67208

W. E. Heronemus
Department of Civil Engineering
University of Massachusetts
Amherst, MA 01002

TID-4500-R61, UC13 (143)

1540 T. B. Lane
1544 W. N. Sullivan
1544 L. I. Weingarten
3161 J. E. Mitchell (20)
4700 D. B. Shuster
4736 J. F. Banas
5000 A. Narath
5600 A. Y. Pope
5620 R. C. Maydew
5623 E. C. Rightley
5623 L. V. Feltz
5628 S. McAlees, Jr.
5644 J. W. Reed
5700 J. H. Scott
5710 G. E. Brandvold
5712 R. H. Braasch
5712 E. G. Kadlec (50)
5712 R. C. Reuter
5712 A. F. Veneruso
8100 L. Gutierrez
8110 A. N. Blackwell
3141 L. S. Ostrander (5)
3151 W. L. Garner (3)
For ERDA/TIC
(Unlimited Release)
8266 E. A. Aas (2)

☆ U.S. GOVERNMENT PRINTING OFFICE 1978—777-090/513